Eur. Phys. J. B **19**, 501–505 (2001)

THE EUROPEAN PHYSICAL JOURNAL B

EDP Sciences

Evidence for a compressed fluid phase of Xe clusters

F. Zontone[1], F. D'Acapito[2], G. Faraci[3,a], and A.R. Pennisi[3]

[1] ESRF, European Synchrotron Research Facility, BP 220, 38043 Grenoble Cedex, France
[2] INFM-OGG, c/o ESRF GILDA CRG, European Synchrotron Research Facility, BP 220, 38043 Grenoble Cedex, France
[3] Dipartimento di Fisica, Università di Catania, Istituto Nazionale di Fisica della Materia, Unità di Catania, Corso Italia 57, 95129 Catania, Italy

Received 4 September 2000 and Received in final form 13 December 2000

Abstract. We report on the formation and detection of a compressed fluid phase of Xe clusters in as-implanted Si, at room temperature. The simultaneous structural characterization of the Xe clusters and of the Si matrix was performed by X-ray diffraction at grazing incidence coupled with two-dimensional detection; in both cases, the nearest-neighbor distance and the coordination were obtained. In order to investigate the early stage of the atomic inclusion and the cluster segregation, the average compression and size of Xe fluid clusters within the amorphous Si matrix were explained within the simple Hard Sphere model.

PACS. 36.40.-c Atomic and molecular clusters – 61.43.-j Disordered solids – 61.25.Bi Liquid noble gases

As it is well known, rare gas clusters can be formed in a metal or semiconductor by means of ion implantation [1–11]. These clusters can be found in the solid phase, often epitaxially aligned with the matrix and therefore crystalline and overpressurized by the large pressure exerted by the host lattice. Many parameters such as the implant ion fluence and temperature, the thermal treatment of the implanted sample and the matrix configuration play an important role in the growth of these agglomerates. The early phase configuration of the rare gas in the as-implanted sample is still not clear: whereas for light rare gases such as Ne or Ar, solid clusters were detected prior to any annealing [5,7–9], for the heavier ones, Kr and Xe, many efforts seeking to investigate the initial agglomeration stage in the as-implanted matrices, failed [2,4,10,11]. In these cases, *e.g.*, no EXAFS (Extended X-ray Absorption Fine Structure) oscillations were detected [2,4], although clear evidence of rare gas clustering was sometimes obtained [4].

Furthermore, it is also quite controversial whether the cluster segregation and confinement can be obtained in the early stage of the atomic inclusion or whether it is driven only by a thermal treatment in crystalline or amorphous phase: in fact, the cluster configuration can be dramatically dependent on the matrix phase, whenever the implantation process induces the amorphization of the substrate along the ion path. This is the case of a Si crystal implanted at RT, whereas metals [4] remain in crystal phase after implantation.

Of course, the limited experimental resolution can represent an obstacle towards the detection of subtle effects. In this paper, we report on a successful investigation of Xe as-implanted Si: for the first time, we obtained the X-ray structural characterization of Xe clusters (including nearest- neighbor (nn) distance and coordination) showing evidence for the formation of a Xe compressed fluid phase prior to any annealing. Also the Si matrix was simultaneously checked and verified to be in an amorphous phase; here too, nn distance and coordination were measured. The simultaneous characterization of both the matrix and the Xe inclusions was possible using a new X-ray diffraction method which combines grazing incidence geometry, highly collimated, very intense Synchrotron Radiation beams and two-dimensional detection. This method permitted the maximization of the implanted thin layer contribution [12–14]. Here, we compare an X-ray diffraction study of two Si samples, one implanted at high fluence (10^{17} at/cm^2 at 350 keV, labelled "H") and the other implanted at a lower fluence (1.5×10^{16} at/cm^2 at 200 keV, labelled "L").

In these conditions the implantation profile has a Gaussian shape centered at about 1000 Å below the matrix surface [15]. In order to maximize the scattering from the buried layer rich in Xe we used the grazing incidence geometry near the critical angle for total external reflection ($\approx 0.1°$). The experiments were performed at the European Synchrotron Radiation Facility on beamline ID09. An extensive description of the experimental arrangement can be found in references [12,14]. The grazing angle is chosen by looking at the reflectivity curve of the sample. The presence of the rare gas-rich layer is revealed

[a] e-mail: giuseppe.faraci@ct.infn.it

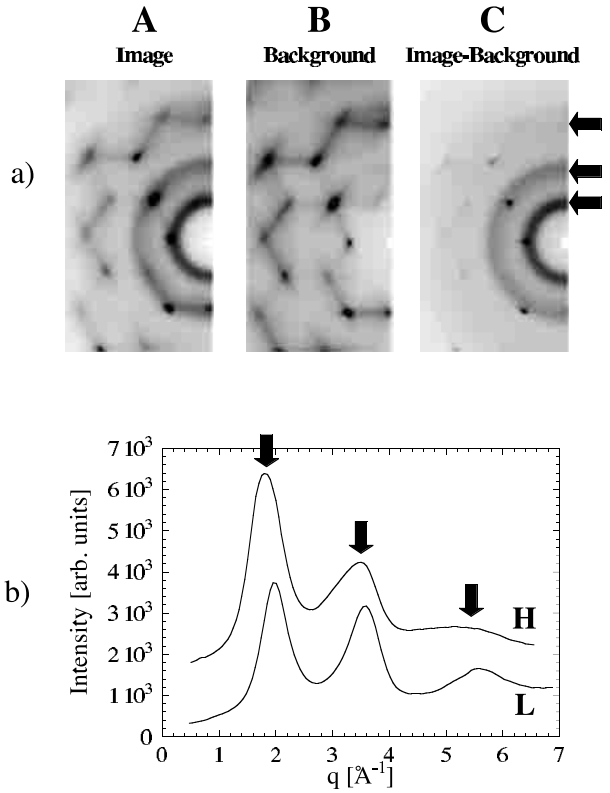

Fig. 1. (a) Diffraction image (A) and background (B) of the sample H: the background (B) obtained from the non-implanted part of the sample is subtracted from the original image (A) to obtain the difference image (C). In the difference image the arrows show the diffuse rings produced by the amorphous phases present in the buried implanted layer. (b) Raw intensity functions $I(q)$ of the investigated samples obtained from the azimuthal integration of the difference images.

by a step above the critical angle for the air-Si interface. Here, we set the grazing angle and we collected the diffraction pattern onto flat imaging plates (IP) placed at normal incidence at 344 mm from the sample with an integration time of two minutes. The working X-ray wavelength was $\lambda = 0.4618$ Å. The quantity of implanted material corresponds to few monolayers in equivalent thickness, therefore, the diffraction patterns consist of the weak scattering signal from the Xe-rich layer superimposed on the scattering from the single crystal matrix, *i.e.* Bragg spots, Thermal Diffuse Scattering (TDS) and Compton radiation (image A in Fig. 1a). This highly patterned background is subtracted directly in the image by taking a reference background pattern of the non-implanted part of the sample in the same grazing incidence condition (image B in Fig. 1a). The result is shown in image C of Figure 1a for sample H. In the background image the main feature is the hexagonal distribution of diffuse radiation coming from the (acoustic) phonon scattering. Since the intensity of the TDS has a linear dependence on the volume we have scaled the background pattern in order to obtain a difference image with the minimum TDS contribution. The extra features still visible in the difference image are mainly coming from saturated regions of the IP. The difference pattern shows diffuse rings at $q \approx 2$ Å^{-1} and $q \approx 4$ Å^{-1} (q being the exchanged momentum $4\pi \sin(\theta/2)/\lambda$ at the scattering angle θ) which are produced by the amorphous phases formed in the buried layer damaged by the ion bombardment [16]. An azimuthal integration is then performed in order to obtain the intensity function $I(q)$ after having masked the residual extra features in the difference image. These are shown in Figure 1b for both samples. The intensity functions are remarkably different in the two samples; in particular, the first peak is much higher than the second one in sample H. This fact suggests either a strong structural change in the amorphized Si phase when implanted at higher doses or more likely the appearance of a disordered phase related to the implanted Xe. To test these hypotheses we applied the standard analysis for X-ray scattering data from disordered systems (see, *e.g.*, Ref. [17]) supposing at start the presence of the Si amorphous phase (a-Si) only. This procedure consists in converting the elastically scattered part of the scattering intensity into electron units, $I_{\rm eu}$, calculating the structure function $S(q)$ from:

$$S(q) = \frac{I_{\rm eu} - f^2(q)}{f^2(q)} \tag{1}$$

where $f(q)$ is the Xe atomic scattering factor. The $S(q)$ contains already all the structural information we are looking for, but very often a Fourier Transform is performed to obtain the pair correlation function $G(r)$ which gives direct access to the structural information such as coordination distances and coordination numbers, *i.e.*,

$$G(r) = 1 + \frac{1}{2\pi^2 r \rho_0} \int_0^\infty qS(q) \sin(qr) \mathrm{d}q \tag{2}$$

ρ_0 being the site density of the material.

Both functions $S(q)$ and $G(r)$ can be used to structurally characterize a disordered system, depending on the q-range and quality of the data as well as on the system itself. In the limited q-range ($q_{\max} \approx 7$ Å^{-1}) the functions $G(r)$ can be efficiently used to extract accurate structural parameters especially by comparison with literature data. The functions $S(q)$ and $G(r)$ for both sample are shown in Figure 2. The $G(r)$ has often a spurious peak at small r values caused by small "low frequency" errors in $S(q)$ produced in the data treatment (normalization, background subtraction, etc.) A very effective method to correct for such errors is a refinement procedure based on a Fourier transform where $G(r) - 1$ is reinverted with a cut-off at a fixed r value to give the corrected $S(q)$. This method was applied to sample L where the a-Si phase is clearly recognizable, whereas for sample H the unrefined $S(q)$ and $G(r)$ are presented. In both cases the data were extrapolated in the missing region around $q = 0$. The $S(q)$ and $G(r)$ obtained with the refining procedure described above are compared with literature X-ray data derived from reference [18], as shown in Figure 2. The comparison clearly demonstrates the presence of the a-Si phase characterized by a 3-dimensional random network of tetrahedrally

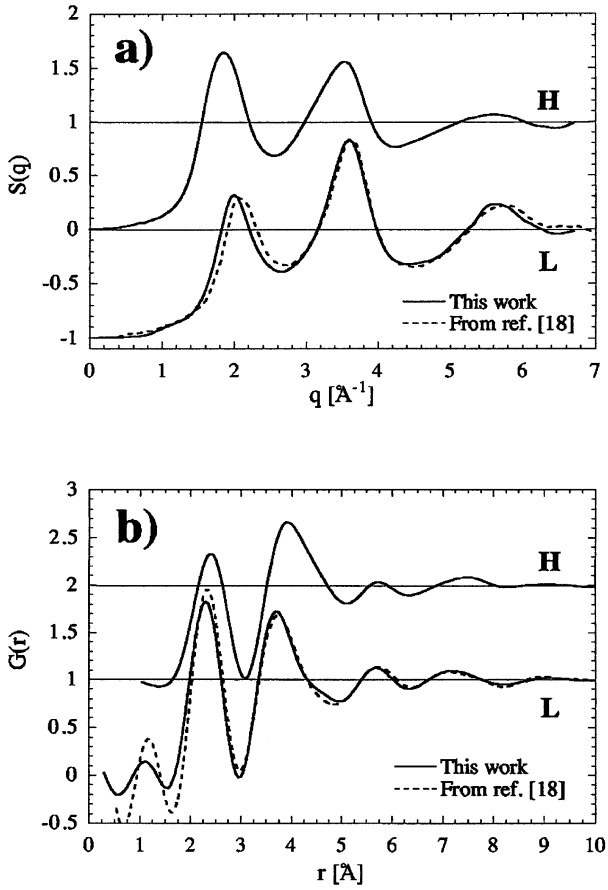

Fig. 2. Experimental functions (a) $S(q)$, (b) $G(r)$ obtained by considering the presence of the a-Si phase only. The curves of the sample L are compared with the a-Si phase obtained from reference [18].

bonded atoms. The first and second neighbor distances are $R_1 = 2.38(1)$ Å and $R_2 = 3.78(1)$ Å respectively, very close to those reported in reference [18] ($R_1 = 2.36$ Å, $R_2 = 3.77$ Å by using the same fitting procedure). The small deviations observed mainly in the $S(q)$ can be likely ascribed to the different sample preparation and/or to the influence of the Xe in the damaged Si matrix. The results show a remarkably different situation for the sample implanted at higher dose. The $I(q)$ and $S(q)$ show both a redistribution of the intensity and a change of the peak positions (see Fig. 1). This causes in the $G(r)$ a noticeable decreasing amplitude of the peaks at 2.3 Å and 5.7 Å and a displacement of the second peak closer to 4 Å (see Fig. 2). Since Si and Xe are non-miscible, we are actually observing the coexistence of two phases: the previous a-Si phase plus a disordered condensed phase of the implanted Xe. To prove such hypotheses we have subtracted the a-Si phase as obtained from the sample L in the intensity function of the sample H in order to minimize the peaks in the $G(r)$ at 2.3 Å and at 5.7 Å which should be ascribed to the a-Si only. The result of the subtraction is shown in Figure 3 where we can easily recognize a simple-liquid like intensity function. The intensity function obtained for the Xe phase was treated in the same way as previously

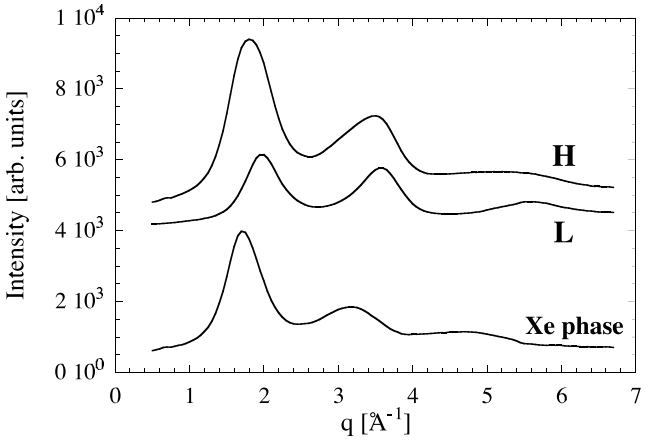

Fig. 3. The extraction of the intensity function of the Xe phase as obtained by subtracting the a-Si phase of the sample L from the sample H. For clarity the curves H and L are vertically shifted.

described to get the $S(q)$. Since in rare gas systems the interaction is of Van der Waals type, the $S(q)$ was interpreted in terms of the Hard-Sphere model and compared with literature data. A known solution of this model is the Percus-Yevick integral equation which gives a simple form of the liquid structure factor for a system of spheres of diameter D which depends only on the effective packing density of the fluid (see Ref. [19] and references therein),

$$S(q) + 1 = \frac{1}{1 - \rho_0 Z(q)} \tag{3}$$

where $Z(q)$ is given by

$$Z(q) = -4\pi D^3 \int_0^1 s^2 \frac{\sin(sqD)}{sqD}(a + bs + cs^2)\mathrm{d}s \tag{4}$$

a, b and c are functions of the packing density parameter η, the fraction of the total fluid volume occupied by the spheres:

$$\begin{aligned} \eta &= (\pi/6)\rho_0 D^3 \\ a &= (1 + 2\eta)2/(1 - \eta)^4 \\ b &= -6\eta\,(1 + \eta/2)^2/(1 - \eta)^4 \\ c &= -(1/2)\eta\,(1 + 2\eta)^2/(1 - \eta)^4. \end{aligned} \tag{5}$$

We have firstly applied the model to X-ray data for liquid Xe near the triple point obtained from reference [20]. In Figure 4 is shown the fit of the structure function with equation (3) having D and η as free parameters. With spheres of $D = 4.094$ Å which occupy a volume fraction $\eta = 0.478$ we can reproduce the main features in the $S(q)$ (Fig. 4a) and account for the pair correlation function having ≈ 9 first neighbors at a distance about 4.37 Å (Fig. 4b). We attribute the apparent sharper modulations of the model mainly to the lack of momentum resolution in the literature data. The same model applied to our structure function is shown in Figure 4c.

The HS model reproduces the experimental $S(q)$ even better than in the previous example with significantly

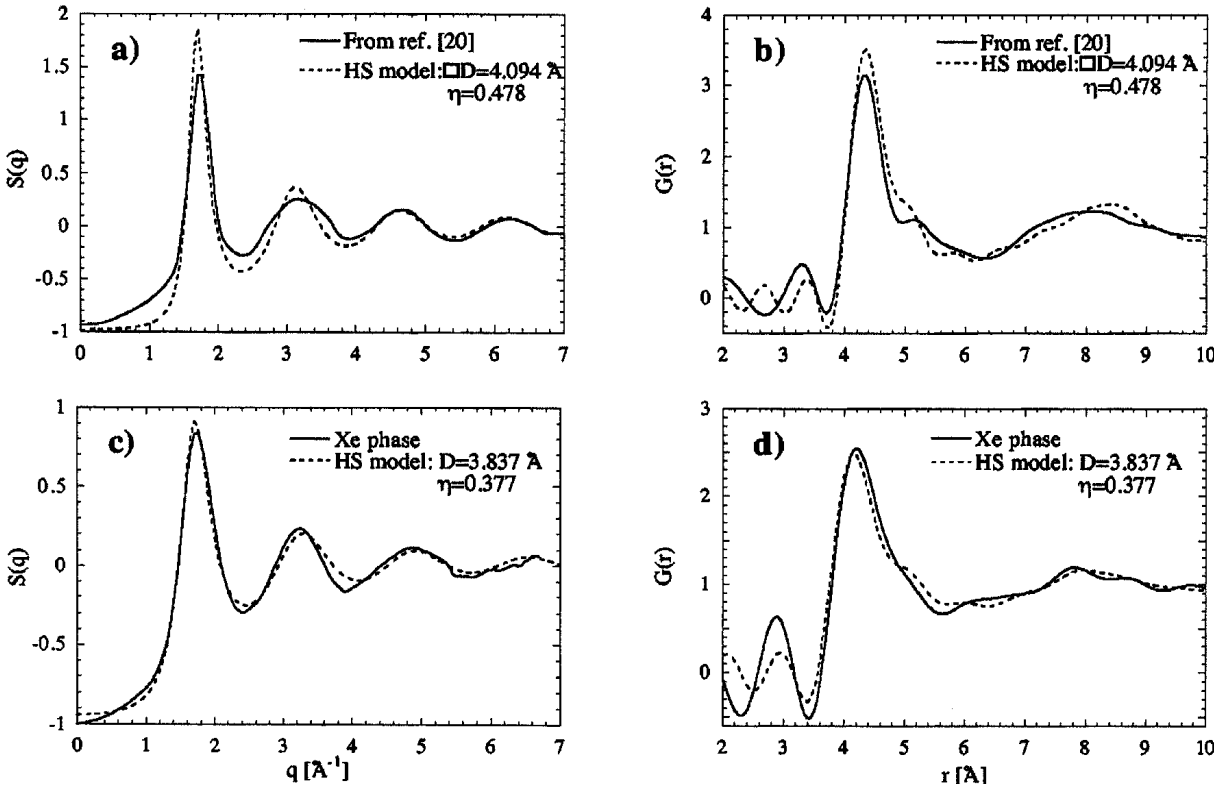

Fig. 4. The HS model applied to the $S(q)$ for (a) liquid Xe at the triple point (data from Ref. [20]), (b) the correspondent $G(r)$. (c) and (d) as above, for our data.

Table 1. Comparison of the structural parameters as obtained from a Gaussian fit of the 1st peak in the $4\pi r^2 G(r)$ and from the Hard-Sphere model.

	1st neigh. dist. [Å]	1st coord. n.	D [Å]	η
Liquid Xe	4.37 ± 0.01	9 ± 1	4.094 (0.005)	0.478 (0.005)
Xe clusters	4.22 ± 0.01	6 ± 1	3.837 (0.005)	0.377 (0.005)

smaller values for the sphere diameter (D = 3.837 Å) and the volume fraction η = 0.377. These reduced values confirm the presence of a Xe fluid phase. A smaller sphere diameter and a reduced volume fraction (Tab. 1) account for a $G(r)$ having a broader first peak at a shorter distance of about 4.22 Å (Fig. 4d). A reduced first neighbor distance implies an overpressurized state related to nanometer sized particles.

We emphasize that the lattice contraction is here assumed as a consequence of the overpressurization; strictly speaking, an overpressure on the clusters should be referred to the equilibrium pressure, which, for a spherical particle in a Si matrix, is of the order of $2\gamma/R$ where γ is the silicon surface tension and R the particle radius.

Such compression in small particles due to the surface stress is a very well known effect [21]. The small size of the particles could also explain the 20% reduction in volume fraction, *i.e.*, the high surface-to-volume ratio could be responsible for the reduced average coordination number with respect to the usual liquid state. We therefore believe to have evidence of a disordered condensed phase for implanted Xe formed by small fluid bubbles in an overpressurized state. Using the average coordination, the volume and surface density of solid Xe we can now estimate the average diameter of these Xe bubbles [22] as about 20 Å, with a pressure acting on the bubbles of the order of 1 GPa [11], a value comparable to the pressure at the liquid-solid phase transition at room temperature (0.43 GPa [23]); whereas, assuming for Si the value $\gamma = 0.625$ J/m^2 [10] we obtain an equilibrium pressure of 1.25 GPa; note that the non-uniform size of the clusters causes an uncertainty lower than 10%.

It is certainly true that the Percus-Yevick equation just describes the random packing of rigid spheres in close contact. Therefore, such approximation should be sufficiently accurate for the high density systems such as those we are treating in the present paper. However, for dilute systems (let's say η =0.1–0.2) an attractive potential might be included for a better description of the $S(q)$.

We have tried to include this attractive term in our fit by taking as solution for the $S(q)$ the potential given in reference [24]. The fit model considers two additional

parameters, *i.e.* the depth ε of the well (in units of $k_{\rm B}T$) and the width δ (in units of D plus 1). The fitted parameters are:

$$D = 3.844 \text{ Å}; \qquad \eta = 0.370$$
$$\varepsilon = 0.225; \qquad \delta = 1.20.$$

The values found for D and η with the Sharma model [24] are very close to those obtained with the simple Hard-Sphere model and therefore the conclusions of the present manuscript are confirmed.

It is worth pointing out the result of a Xe cluster ensemble as a condensed disordered phase since the data do not show any long range order as found, *e.g.*, in crystalline agglomerates where a second and third coordination shell is visible; the clusters are therefore fluid (or in an equivalent configuration, amorphous as the Si matrix), and somewhat pressurized since the nn distance results contracted with respect to a Xe crystal at low temperature. Another possible interpretation of the present data could suggest an ensemble of solid Xe crystallites randomly oriented; in fact, nanocrystallites should give broadened diffraction rings similar to those observed in the present paper. However, the diffraction pattern should distinguish a fluid (or amorphous) phase from that of solid crystallites owing to some longer range order absent in the fluid.

In conclusion, we studied Xe in as-implanted Si crystals by means of grazing incidence X-ray diffraction and area detectors. By a proper choice of the grazing angle it is possible to maximize the scattering from the Xe-rich buried layer with respect to the matrix contribution. All the extracted intensity functions come from amorphous phases. In samples implanted at lower dose we have found the well known intensity function from the a-Si phase which is produced by the ion bombardment. In the "high dose" implanted sample we have observed an excess in the scattering which we ascribe to the implanted Xe. By subtracting the a-Si phase we could extract a liquid-like structure function which has been interpreted in the frame of the Hard-Sphere model. The fitted structural parameters show a 3% contraction in the first neighbor distance and a 20% reduction in the volume fraction with respect to the Xe liquid phase at the triple point. We interpret the results as due to a condensed disordered phase of the Xe formed by an aggregate of nanometer-sized fluid bubbles in a overpressurized state. This phase constitutes the very early stage of the agglomeration of the Xe atoms in a condensed state which takes place during the implantation process.

We wish to acknowledge the staff of ESRF for the excellent assistance during the experiments.

References

1. A. vom Felde, J. Fink, Th. Müller-Heinzerling, J. Pflüger, B. Scheerer, G. Linker, D. Kaletta, Phys. Rev. Lett. **53**, 922 (1984); E. Fleischer, M.G. Norton, Heterog. Chem. Rev. **3**, 171 (1996).
2. G. Faraci, A.R. Pennisi, A. Terrasi, S. Mobilio, Phys. Rev. B **38**, 13468 (1988); G. Faraci, in *Fundamental Aspects of Inert Gases in Solids, Nato ASI Series*, edited by S.E. Donnelly, J.H. Evans (1991), Vol. 279, p. 251.
3. G. Faraci, S. La Rosa, A.R. Pennisi, S. Mobilio, G. Tourillon, Phys. Rev. B **43**, 9962 (1991).
4. G. Faraci, A.R. Pennisi, J.L. Hazemann, Phys. Rev. B **56**, 12553 (1997); A. Polian, J.P. Itie, E. Dartyge, A. Fontaine, G. Tourillon, Phys. Rev. B **39**, 3369 (1989); H.H. Andersen, J. Bohr, A. Johansen, E. Johnson, L. Sarholt-Kristensen, V. Surganov, Phys. Rev. Lett. **59**, 1589 (1987).
5. C.J. Rossouw, S.E. Donnelly, Phys. Rev. Lett. **55**, 2960 (1985).
6. R.C. Birtcher, W. Jaeger, J. Nucl. Mater. **135**, 274 (1985); see also R.C. Birtcher in *Fundamental Aspects of Inert Gases in Solids, Nato ASI Series*, edited by S.E. Donnelly, J.H. Evans (1991) Vol. 279, p. 133.
7. P. Revesz, M. Wittmer, J. Roth, J.W. Mayer, J. Appl. Phys. **49**, 5199 (1978).
8. M. Wittmer, J. Roth, J.W. Mayer, J. Appl. Phys. **49**, 5207 (1978).
9. A. Luukkainen, J. Keinonen, A. Erola, Phys. Rev. B **32**, 4814 (1985).
10. C. Templier, B. Boubeker, H. Garem, E.L. Mathé, J.C. Desoyer, Phys. Stat. Sol. (a) **92**, 511 (1985).
11. J.C. Desoyer, C. Templier, J. Delafond, H. Garem, Nucl. Instr. Methods B **19/20**, 450 (1987); C. Templier, H. Garem, J.P. Riviere, Phil. Mag. A **53**, 667 (1986).
12. F. D'Acapito, D. Thiaudiere, F. Zontone, J.R. Regnard, Mat. Science Forum, **278-281**, 891 (1998).
13. F. Zontone, F. D'Acapito, F. Gonella, Nucl. Instr. Meth. Phys. Res. B **147**, 416 (1999).
14. F. D'Acapito, F. Zontone, J. Appl. Cryst. **32**, 234 (1999).
15. J.P. Biersack, L. Haggmark, Nucl. Instr. Meth. Phys. Res. **174**, 257 (1980).
16. G. Mueller, S. Kalbitzer, Phil. Mag. B **41**, 307 (1980).
17. B.E. Warren, in *X-ray Diffraction* (Addison-Wesley, Reading, Mass., 1969).
18. S. Minomura, K. Tsuji, J. Non-Cryst. Solids **35-36**, 513 (1980).
19. N.W. Aschroft, J. Lekner, Phys. Rev. **145**, 83 (1966).
20. R.W. Harris, G.T. Clayton, Phys. Rev. **153**, 229 (1967).
21. C.W. Mays, J.S. Vermaak, D. Kuhlmann-Wilsdorf, Surf. Sci. **12**, 128 (1968).
22. A. Pinto, A.R. Pennisi, G. Faraci, G. D'Agostino, S. Mobilio, F. Boscherini, Phys. Rev. B **51**, 5315 (1995).
23. F.H. Ree, in *Molecular Systems under High Pressure*, edited by R. Pucci, G. Piccitto, (North Holland, 1991), p. 33.
24. R.V. Sharma, K.C. Sharma, Physica A **89**, 213 (1977).